

Bright-Blood Delayed Contrast-Enhanced Imaging for Improving the CNR between Endocardial Scar and Blood

D. Kim¹, M. B. Srichai¹, V. S. Lee¹

¹Radiology, New York University, New York, New York, United States

Introduction

Delayed contrast-enhanced (DCE) imaging is becoming a clinically acceptable diagnostic method for assessing the extent of myocardial scar [1]. This inversion-recovery (IR) technique exhibits good contrast-to-noise ratio (CNR) between scar and normal myocardium, when the inversion time (TI) is selected to null the signal of the normal myocardium. However, the CNR between blood and endocardial scar is frequently poor, because the T1 values of blood and scar at the time of DCE imaging are similar. This limitation may lead to incorrect estimation of the infarct size and obscure the visualization of small endocardial scar. The dual inversion subtraction [2] and dual contrast [3] methods can be used to improve the CNR between blood and scar, without compromising the CNR between scar and normal myocardium. However, they require two data acquisitions. The purpose of this study was to develop a single acquisition bright-blood DSE pulse sequence for improving the CNR between blood and endocardial scar.

Methods

The bright-blood DCE sequence is based on applying a slice-selective (SS) IR (3x slice thickness) pulse instead of the non-selective (NS) IR pulse (Fig. 1), in order to exploit the benefits of inflow effects for increasing the blood signal. Immediately after the SS IR pulse, the magnetization of scar and normal myocardium undergoes T1 relaxation as in conventional NS IR sequence. During the TI period (~ 320 ms), uninverted blood spins enters the slice and mixes with the inverted blood spins leaving the slice. Assuming T1 values of 300 ms, 460 ms, and 320 ms for scar, normal myocardium, and blood, respectively, 15 minutes post Gd-DTPA injection at 3T, the calculated M/M0 values in an ideal IR experiment at TI = 320 ms are 0.31 and 0.0 for the scar and normal myocardium, respectively. Blood M/M0 value is expected to be between 0.26 (no inflow) – 1.0 (100% inflow), and is dependent on the blood flow rate through the slice. We scanned 8 patients, without a history of coronary artery disease, who were scheduled for a double dose (0.2

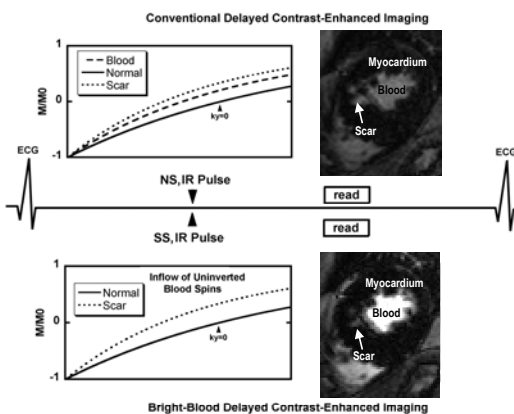


Fig. 1 Pulse sequence of conventional and bright-blood IR sequence

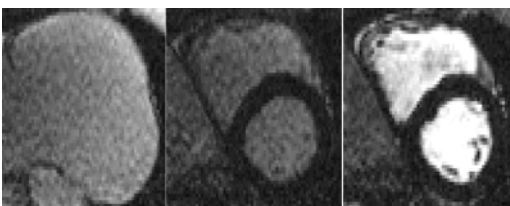


Fig. 2. Representative volunteer delayed contrast-enhanced images: PD (left), conventional (middle), and bright-blood (right) DCE images displayed using identical grayscales (0-120 au).

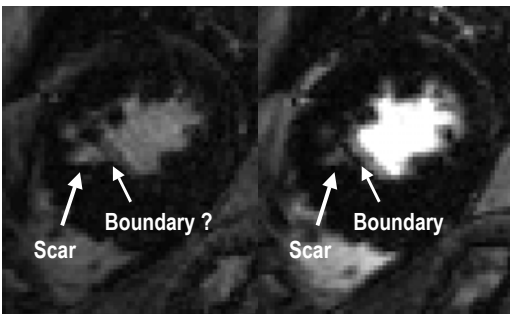


Fig. 3. Representative post-infarct patient images: conventional (left) and bright-blood (right) with identical grayscales.

mmol/kg of 0.5M of Gd-DTPA; Magnevist) contrast MR examination, in order to validate the technique for scanning myocardial infarct patients. An informed consent form was obtained for each patient. The patients were imaged in 3 short-axis views of the left ventricle (LV), using the conventional DSE and bright-blood DSE TurboFLASH imaging with identical imaging parameters, except for the IR pulse. All imaging was performed on a Siemens 3T Tim Trio system using phased array coils. Imaging parameters include: matrix = 192x108, FOV = 340 x 255, flip angle = 10°, BW = 1000 Hz/pixel, TE = 1ms, TR = 1.7ms, slice thickness = 6mm, GRAPPA parallel imaging (R=2), acquisition time = 110 ms, TI = 320-400 ms. An optimized TI scout sequence was used 15-20 minutes post Gd-DTPA injection to determine the TI value to null the myocardial signal [4]. Proton density (PD) images were acquired at identical locations, with no IR pulse and with flip angle of 4°, in order to correct for signal non-uniformity due to receive coil effects and to calibrate the signal to equilibrium magnetization (Fig. 2 displays a representative PD image). The normalized image (M/M0) was calculated by dividing the T1-weighted image by the PD weighted image. The SNR values of the entire LV and region of interest (ROI) of the blood were calculated. The CNR between blood and myocardium was calculated. The mean normalized signal was calculated for the entire LV and blood, as well as the signal difference between blood and myocardium. One post-infarct patient was scanned at multiple views of the heart, using bright-blood DSE and conventional DSE imaging.

Results

For patient data without scar (Fig. 2), SNR and the corresponding normalized signal values of the myocardium were not different between bright-blood DSE and conventional DSE imaging (5.4 vs 5.4; 0.09 vs 0.09; $p < 0.001$). The CNR and normalized signal difference values between blood and myocardium were significantly higher for the bright-blood DSE than for conventional DSE imaging (40.4 vs 8.4; 0.13 vs 0.62; $p < 0.001$). For the infarct patient (Fig. 3), SNR of uninfarcted myocardium was not different between bright-blood DSE and conventional DSE imaging (5.6 vs 5.4), but the corresponding CNR between blood and endocardial scar was higher for the bright-blood DSE than for conventional DSE imaging (97.4 vs 26.7). For the bright-blood DSE image in Fig. 3, the dark rim (as in myocardial first-pass imaging) due to Gibbs ringing artifact delineates the blood-to-endocardium boundary.

Discussion

We have demonstrated the feasibility of using the bright-blood DSE sequence for improving the CNR between blood and endocardial scar. While this technique was implemented on a TurboFLASH sequence, it can also be implemented on segmented FLASH, segmented TrueFisp, and single-shot TrueFisp. This technique does not perform well for long-axis imaging of the heart, because the increase signal from inflow effects is minimal when the flow is predominantly in-plane. Combination of partial volume effects and inflow effects due to slow-flowing blood at the endocardium border may obscure the visualization of small subendocardial scar, but this limitation is also a problem for conventional DSE, dual inversion DSE, and dual contrast DSE imaging.

References:

1. Kim, R.J, et al. *Circulation* 100:1992-2002 (1999).
2. Foo, TKF et al. *Magn Reson Med* 53:1484-1489 (2005).
3. Kellman, P et al. *JMRI* 22:605-613 (2005).
4. Gupta, A et al. *Radiology* 233: 921-926 (2004).